Journal of Pharmaceutical Innovation (2026) 21:578
https://doi.org/10.1007/s12247-026-10789-3

RESEARCH

Paroxetine HCl-Loaded Polymeric Nanoparticles for Colorectal Cancer Therapy: Optimization by Box–Behnken Design and Evaluation of Antiproliferative Efficiency on HCT-116 Cells

Semra Durak[1,2] · **Ozge Esim**[3] · **Aslı Koc**[4] · **Canan Hascicek**[3,5]

Received: 11 February 2026 / Accepted: 1 June 2026
© The Author(s) 2026

Abstract

Purpose Colorectal cancer (CRC) continues to be one of the leading causes of cancer-related deaths, and current chemotherapeutic regimens face significant limitations such as systemic toxicity, limited tumor specificity and multidrug resistance. To overcome these limitations, the combination of drug repurposing with nanoscale drug-delivery platforms is an innovative approach to enhance therapeutic efficacy while improving safety. In this study, the antiproliferative potential of paroxetine HCl, a selective serotonin reuptake inhibitor (SSRI), is aimed to be evaluated in the context of CRC treatment through polycaprolactone (PCL) nanoparticles.

Methods Paroxetine HCl-loaded polymeric nanoparticles were prepared using the double emulsion-solvent evaporation method. Formulation parameters were systematically optimized using a Box–Behnken experimental design, and the nanoparticles were characterized for their physicochemical properties. The cytotoxicity of the nanoparticles was investigated in vitro using the HCT-116 CRC cell line.

Results Optimized nanoparticles exhibited an average particle size of 304.1 ± 1.76 nm, a polydispersity index of 0.143 ± 0.014 and an an encapsulation efficiency of 88%. In vitro release studies indicated a sustained release profile above 88% over 12 h. Cytotoxicity tests conducted on HCT-116 cells have revealed that the nanoparticle formulation exhibits a significantly greater antiproliferative effect than free paroxetine HCl.

Conclusion The findings indicate that paroxetine HCl-loaded polymeric nanoparticles offer a promising drug-repositioning and nanocarrier strategy for the treatment of CRC. However, comprehensive in vivo and advanced preclinical studies are needed to validate the clinical applicability of this system.

✉ Canan Hascicek
cogan@pharmacy.ankara.edu.tr

Semra Durak
s.durak@firat.edu.tr

Ozge Esim
gun@ankara.edu.tr

Aslı Koc
akoc@ankara.edu.tr

[1] Department of Pharmaceutical Technology, Faculty of Pharmacy, Fırat University, Elazığ, Turkey

[2] Graduate School of Health Sciences, Ankara University, Ankara, Turkey

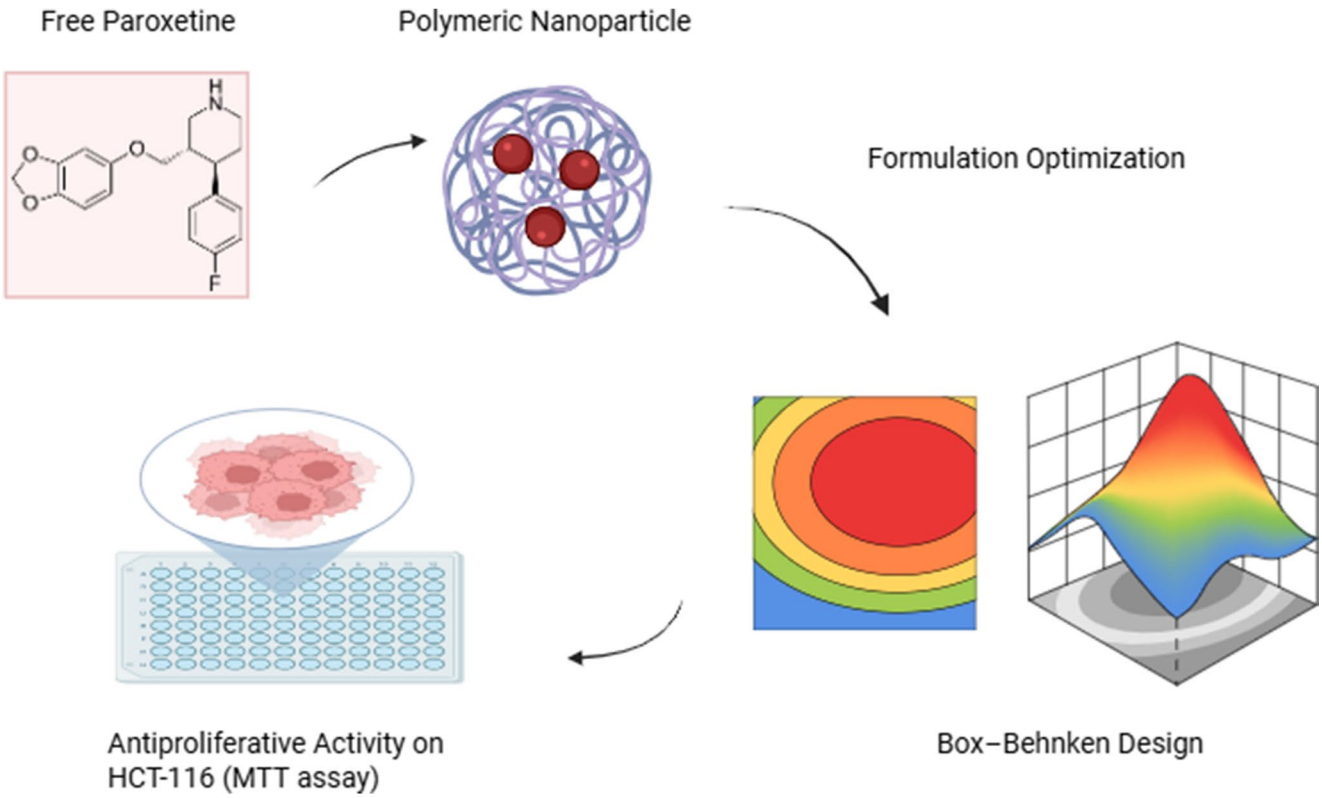
[3] Department of Pharmaceutical Technology, Faculty of Pharmacy, Ankara University, Ankara, Turkey

[4] Department of Biochemistry, Faculty of Pharmacy, Ankara University, Ankara, Turkey

[5] Department of Pharmaceutical Technology, Faculty of Pharmacy, Ankara University, Ankara 06560, Turkey

Published online: 12 June 2026

Graphical Abstract



Keywords box behnken design · colorectal cancer · nanoparticles · paroxetine HCL · repurposing

Introduction

CRC is one of the most common malignancies globally and poses a serious public health problem in terms of both incidence and mortality rates [1]. According to the World Health Organization's 2026 updated colorectal cancer data, colorectal cancer is one of the most commonly observed malignancies worldwide and is among the leading causes of cancer-related deaths. Especially in individuals under 50 years of age, a significant increase in the incidence and mortality of colorectal cancer has been reported [2]. Current standard treatment strategies consist of surgical resection, chemotherapy, radiotherapy, and targeted therapies, with systemic chemotherapy playing a particularly important role in metastatic disease [3, 4]. While current chemotherapeutic regimens are effective in inhibiting tumor growth, they have the potential for serious side effects. Limited drug delivery to tumor tissue, low selectivity for healthy cells, the development of multidrug resistance, and cancer cell evasion of apoptosis mechanisms significantly limit treatment success [3, 4]. Furthermore, chemotherapy-induced adverse effects such as mucositis, neurotoxicity, and myelosuppression reduce patients' quality of life and negatively effect the treatment compliance [5, 6]. Therefore, the development of innovative drug delivery systems that increase tumor-targeting efficacy while reducing systemic toxicity in CRC treatment is critical [7, 8].

Recently, drug repurposing strategies in cancer treatment have become an important area of research [9, 10]. This approach allows the use of licensed drugs with well-known safety profiles in different indications, thereby reducing the time and cost of clinical development. Selective serotonin reuptake inhibitors have been used in clinical psychiatry since the late 1980s as first-line agents for the treatment of major depressive and anxiety disorders. In recent years, growing evidence has suggested that these agents may also exert antitumor and cytotoxic effects through mechanisms independent of serotonergic modulation, drawing significant attention in oncology research [11–13]. Among them, paroxetine HCl (PRX), a potent SSRI, enhances serotonergic neurotransmission by inhibiting the serotonin transporter, thereby increasing extracellular serotonin levels in the synaptic cleft [14, 15]. Preclinical research indicates that PRX can induce programmed cell death in various cancer cell

models and inhibit tumor cell growth. Huang et al. (2024) demonstrated that PRX disrupts autophagic flux in triple-negative breast cancer cells, leading to disruption of cellular homeostasis and inhibition of apoptotic cell death [16]. Similarly, Cho et al. (2019) reported that paroxetine treatment increased p38 MAPK-mediated reactive oxygen species (ROS) production in MCF-7 breast cancer cells, thereby activating its cytotoxic pathway [17]. Beyond breast cancer models, paroxetine has also been reported to show similar antiproliferative effects in colon and lung cancer cells. While Jang et al. (2018) demonstrated that suppression of MET and ERBB3 signaling in colon cancer cells inhibited the AKT and ERK pathways and induced apoptosis [18], Wang et al. (2020) reported that impaired autophagy flux in lung cancer cells triggered cell death through mitochondrial dysfunction and ROS-MAPK activation [19]. Additionally, the increase in genomic stress through the suppression of DNA repair proteins in gastric cancer cells has been identified as another mechanism contributing to the cytotoxic effects of paroxetine [20]. When evaluating data from these various tumor models, it is evident that paroxetine's anticancer effects extend beyond serotonergic modulation. It interacts with mitochondrial function, the balance of Bcl-2 family proteins, and cellular survival pathways such as PI3K/AKT. Although antiproliferative properties of PRX have been extensively studied in breast cancer and several other tumors, its effects on CRC are yet to be fully understood. This represents a significant knowledge gap, particularly given the clinical challenges associated with CRC management. Standard chemotherapeutic strategies for CRC are frequently constrained by cumulative toxicity, the emergence of drug resistance, and suboptimal tumor selectivity, which collectively limit long-term treatment efficacy.

In this context, repurposing clinically validated drugs such as PRX offers a promising approach to broaden therapeutic options. Nevertheless, when administered in its conventional oral form, PRX may exhibit pharmaceutical and pharmacokinetic limitations, including low solubility, insufficient tumor tissue accumulation and unintended systemic exposure. In addition, PRX undergoes extensive hepatic first-pass metabolism, primarily mediated by CYP2D6, which lowers systemic bioavailability and may contribute to variability in therapeutic exposure as well as unintended systemic distribution rather than efficient accumulation in target tissues such as tumors [21–23]. Advances in nanoparticle-based drug delivery platforms address these challenges by stabilizing the drug, promoting cellular internalization, and enhancing drug retention within the tumor microenvironment. Therefore, incorporating PRX into polymeric nanoparticle systems is a logical strategy to enhance its antiproliferative efficacy and expand its potential for CRC therapy.

In this study, PCL was preferred because it is a biocompatible, biodegradable polymer capable of providing controlled drug release [24]. Additionally, the double emulsion-solvent evaporation method was chosen because it is a widely used technique in the preparation of polymeric nanoparticles and can provide suitable particle properties [25].

In the formulation development process, the systematic optimization of formulation and process parameters is crucial to achieving targeted product properties [26]. Conventional single-variable optimization methods require longer time and cost, and they have limitations in identifying potential interactions between variables [27]. To address these shortcomings, experimental design approaches allow to determine the optimum formulation and process parameters by statistically modeling parameter-response relationships [28]. Box–Behnken design (BBD) is a second-order multivariate statistical approach in which independent variables are evaluated at three levels (low, medium, and high). Among these methods, BBD enables reliable predictions with fewer experiments and stands out as an effective tool for simultaneous optimization of multiple response variables, due to its three-level factorial structure [28, 29].

This study aimed to develop a new nanoparticulate drug delivery system loaded with paroxetine HCl for the treatment of CRC. In this context, the paroxetine-loaded polymeric nanoparticles prepared were optimized using the Box–Behnken experimental design. The optimized formulation was then evaluated for antiproliferative activity using the MTT test on the HCT-116 CRC cell line. Based on the obtained findings, the study presents an innovative approach to the evaluation of SSRI-based nanoparticulate systems in CRC treatment.

Materials and Methods

Materials

Paroxetine HCl was kindly provided by Ali Raif Pharmaceutical Industry. Polycaprolactone (PCL, 80 kDa), dichloromethane (DCM), and polyvinyl alcohol (PVA) were purchased from Sigma-Aldrich. RPMI 1640 medium (Euroclone), fetal bovine serum (FBS; Capricorn), penicillin–streptomycin (Capricorn), MTT reagent (Carl Roth), and sodium dodecyl sulfate (SDS; Fluka) were used for cell culture and cytotoxicity assays.

Preparation of PRX-Loaded Polymeric Nanoparticles

PRX-loaded polymeric nanoparticles were prepared using the double emulsion–solvent evaporation method. PRX (1 mg) was dissolved in 1% (w/v) PVA solution as the inner

water phase and sonicated with DCM solution containing PCL to form the primary emulsion (W/O). This emulsion was added to the PVA solution, which was used as the outer phase, under ultrasonication at the determined power and time to obtain the secondary emulsion (W/O/W). The organic solvent was removed by magnetic stirring overnight, and the nanoparticles were collected by centrifugation (Sigma Laboratory Centrifuge 3KS30, Germany) at 20,000 rpm for 40 min. The resulting nanoparticles were redispersed in pure water, frozen, and dried using a lyophilizer (Zirbus VaCo 5, Germany) to obtain the final formulation [30].

All nanoparticle formulations were prepared under the same experimental conditions and using the same method. Sonication parameters, phase volumes, and mixing conditions were kept constant throughout the process. Additionally, the repetition of central points has contributed to the evaluation of experimental variability and the method's repeatability. The physicochemical properties of the formulations were evaluated through independent measurements, and the obtained data were expressed as mean ± standard deviation.

Box–Behnken Design

The Box–Behnken design (BBD) was applied to determine the significance of the independent variables and their interactions, and to obtain the optimum PRX-loaded PCL nanoparticle formulation. Experimental design and statistical analyses were performed using Design-Expert® software (Version 7.0, Stat-Ease Inc., Minneapolis, MN, USA). BBD is a second-order multivariate statistical approach in which independent variables are evaluated at three levels (low, medium, and high). Three independent variables, determined to significantly affect the formulation's physicochemical properties in our preliminary studies, were selected: drug/polymer ratio (X_1), sonication power (X_2), and oil phase volume (X_3). (Table 1). According to the three-factor Box–Behnken design, the experimental matrix consists of 15 different factor combinations and 4 repeated center points for the evaluation of experimental error. Thus, a total of 19 experimental studies were conducted. The repetition of the center point was applied to evaluate the model's goodness of fit, experimental variability, and repeatability.

Table 1 Conditions and constraints in BBD for the optimization of PRX-loaded PCL nanoparticles

Independent variables		Coded levels		
		Low (-1)	Medium (0)	High (+1)
Drug-to-polymer ratio	X_1	1:50	1:100	1:150
Sonication power (W)	X_2	10	20	30
Oil phase volume (ml)	X_3	1.5	3	4.5
Dependent variables		Target		
Particle size (nm)	Y_1	Minimize		
PDI	Y_2	Minimize		
EE (%)	Y_3	Maximize		
% Drug release at 12 h	Y_4	Maximize		

The study aimed to minimize particle size (PS) (Y_1) and polydispersity index (PDI) (Y_2) while maximizing encapsulation efficiency (EE) (Y_3) and the amount of drug released at 12 h (Y_4) (Table 1). The statistical significance and reliability of the model were evaluated by analysis of variance (ANOVA), with $p < 0.05$ considered statistically significant. Model adequacy was further assessed based on the coefficient of determination (R^2), F-statistics, and the correlation between predicted and experimental values. Furthermore, response surface curves were generated to more clearly demonstrate the effects of variables on the responses and to visualize the agreement between experimental and predicted values. These analyses led to the determination of optimum formulation conditions. The conditions were determined using the "desirability" function based on predetermined targets.

Particle Size, Particle Size Distribution, and Zeta Potential Analysis

Particle size and particle size distribution of polymeric nanoparticles were determined by dynamic light scattering, and zeta potential was determined by laser doppler anemometry. Measurements were performed using a Zetasizer (Malvern Instruments, UK) after diluting the nanoparticles with ultrapure water to an appropriate ratio. The results were evaluated in three replicates ($n = 3$).

Encapsulation Efficiency of PRX-loaded Polymeric Nanoparticles

The EE% of PRX-loaded polymeric nanoparticles was determined using indirect method [31]. For this purpose, the supernatants obtained after nanoparticle production were collected by centrifugation, and the amount of free PRX in the supernatant was calculated from absorbance values measured at 293 nm using a developed UV spectrophotometric method [32] ($n = 6$). The results are reported as mean ± standard deviation.

In Vitro Drug Release Studies of Polymeric Nanoparticles

In vitro drug release profiles from PRX-loaded polymeric nanoparticles were evaluated using the dialysis membrane method [33]. Buffer solutions at pH 1.2, pH 4.5, and pH 7.4 (each supplemented with 0.1% Tween 80) were selected as release media to simulate the physiological environments of the gastric, intestinal, and colonic regions, respectively.

After the predetermined amount of lyophilized nanoparticles was dispersed in 2 mL of release medium, the mixture was placed in dialysis membrane tubes (Sigma-Aldrich, Germany) with an molecular weight cutoff (MWCO) of 12 kDa and sealed at both ends. The tubes were immersed in the release medium to a total volume of 30 mL and incubated at 37 ± 0.5 °C in an orbital shaker incubator (Jeio Tech SI-300, Jeio Tech Co. Ltd, South Korea) set at 100 rpm. 1 mL samples were taken at predetermined time intervals, and an equal volume of fresh release medium was added. If necessary, the absorbance of diluted samples in ultrapure water was measured on a UV spectrophotometer at 293 nm. All experiments were performed in triplicate, and release profiles were created by calculating the time-dependent release percentages.

The mathematical modelling of dissolution profile of paroxetine HCl-loaded polymeric nanoparticles was identified using DDSolver™ software [34]. The kinetic model was selected on the basis of best with the highest correlation (r^2) value.

Morphological Evaluation of the Formulation of Optimized Polymeric Nanoparticles

The morphological properties, shape, and potential aggregation of the optimum PRX-loaded polymeric nanoparticles formulation were examined using a transmission electron microscope (TEM) (an FEI Tecnai G² Spirit Biotwin) at 20–120 kV accelerating voltage range, enabling high-contrast imaging of polymeric samples.

Evaluation of the Stability of the Optimized Polymeric Nanoparticles

The stability of the optimized PRX-loaded polymeric nanoparticle formulation that was stored at 4 °C during 3 months was evaluated in terms of physicochemical properties including particle size, PDI and zeta potential.

Cell Culture and MTT Cytotoxicity Assay

The HCT-116 human CRC cell line was cultured in RPMI-1640 medium containing 10% fetal bovine serum (FBS), 1% penicillin/streptomycin, and 1% L-glutamine in 75 cm² culture flasks at 37 °C in a humidified incubator with a 5% CO_2 atmosphere. When the cells reached approximately 80% confluency, they were trypsinized with trypsin-EDTA. The antiproliferative effects of the free PRX and the optimum PRX-loaded polymeric nanoparticles formulation were evaluated using the MTT (3-[4,5-dimethylthiazol-2-yl]-2,5-diphenyltetrazolium bromide) assay [18, 35]. Assays were performed in 96-well cell culture plates, seeding 5 × 10³ cells per well. Cells were incubated overnight at 37 °C in a 5% CO_2 incubator to allow for adherence. The following day, free PRX (0.244–15.625 µg/mL) and the optimum PRX-loaded polymeric nanoparticles formulation (0.059–3.8 µg/mL) were applied to the cells at the specified concentration ranges. After treatment, cells were incubated for 24, 48, and 72 h. At the end of the incubation periods, 5 mg/mL MTT solution dissolved in PBS was added to each well and incubated for 4 h. The resulting formazan crystals were dissolved in the appropriate solvent, and absorbance measurements were performed on a microplate reader at 550 nm. The viability of control group cells was accepted as 100%.

Statistical Analysis

All data are expressed as mean ± standard deviation. Statistical analyses were performed using GraphPad Prism 9 software (GraphPad Software, Inc., San Diego, CA, USA). Data normality was assessed using the Shapiro–Wilk test. Differences between groups with normal distributions were determined using one-way analysis of variance (One-Way ANOVA), and for data not normally distributed, the Kruskal–Wallis test was used. Statistical significance was set at $p < 0.05$.

Results and Discussion

Experimental Design and Optimization Studies

In this study, nineteen PRX-loaded nanoparticles were successfully designed using the Box–Behnken experimental design. The desirable features of the developed PCL-based polymeric nanoparticles are high entrapment efficiency, a narrow particle size distribution, and suitable surface charge and in vitro dissolution. The drug/polymer ratio, sonication power, and the oil phase volume are the determining critical factors for providing the intended features, according to several authors [31].

The average particle sizes of the formulations ranged between 243.0 and 468.5 nm (Table 2). Model analysis confirmed that the linear model was the most appropriate to describe the relationship between the independent variables and particle size ($p < 0.05$). According to the model graphs (Fig. 1) and mathematical expressions (Table 3), particle size was significantly affected ($p < 0.05$) by the drug/polymer ratio (X1) and the oil phase volume (X3). A decrease polymer amount resulted in smaller particles, whereas an increase in the oil phase volume led to larger particles. While keeping the other two factors constant, sonication power (X2) did not significantly affect particle size.

Table 2 Characterization parameters of PRX-loaded nanoparticle formulations optimized via the BBD (mean ± SD)

Code	PS (nm) ± SD	PDI ± SD	Dissolution of 12th hour (%) ± SD	EE ± SD (%)
PRX1	384 ± 6.381	0.352 ± 0.026	99.01 ± 0.520	86.68 ± 0.061
PRX2	243 ± 3.213	0.072 ± 0.048	94.43 ± 0.170	84.24 ± 0.099
PRX3	305.1 ± 1.768	0.275 ± 0.006	78.16 ± 0.370	87.36 ± 0.131
PRX4	343 ± 6.313	0.247 ± 0.009	99.36 ± 0.590	71.71 ± 0.420
PRX5	317 ± 3.329	0.165 ± 0.021	84.13 ± 0.110	86.01 ± 0.015
PRX6	306 ± 3.092	0.242 ± 0.013	29.44 ± 0.280	89.22 ± 0.061
PRX7	293 ± 6.525	0.218 ± 0.037	61.02 ± 0.120	69.86 ± 0.194
PRX8	324 ± 2.107	0.181 ± 0.036	97.64 ± 0.280	88.76 ± 0.073
PRX9	295 ± 3.830	0.181 ± 0.025	88.16 ± 0.450	85.62 ± 0.268
PRX10	257 ± 4.901	0.129 ± 0.006	38.88 ± 0.830	86.16 ± 0.083
PRX11	274 ± 5.220	0.218 ± 0.016	19.22 ± 0.050	77.89 ± 0.038
PRX12	458 ± 47.840	0.596 ± 0.121	28.08 ± 0.050	78.32 ± 0.117
PRX13	381 ± 17.390	0.406 ± 0.007	27.42 ± 0.470	88.25 ± 0.134
PRX14	361 ± 6.404	0.390 ± 0.016	50.56 ± 0.320	87.70 ± 0.166
PRX15	376 ± 6.063	0.282 ± 0.019	56.37 ± 0.180	89.35 ± 0.113
PRX16	359 ± 3.482	0.287 ± 0.028	54.94 ± 0.140	90.51 ± 0.158
PRX17	468.5 ± 15.790	0.597 ± 0.097	36.58 ± 0.150	88.46 ± 0.313
PRX18	367 ± 3.528	0.279 ± 0.024	65.69 ± 0.650	88.91 ± 0.232
PRX19	329.5 ± 3.592	0.276 ± 0.011	36.55 ± 0.500	87.32 ± 0.107

Model graphs and mathematical expressions clearly demonstrate that polymer concentration and oil phase volume significantly influence nanoparticle size. Increasing the polymer content increases the viscosity of the dispersed phase, hindering droplet disruption during emulsification and promoting the retention of larger droplets, ultimately resulting in larger nanoparticles [36] (Fig. 1A-C). Likewise, a higher volume of the oil phase results in larger primary droplets at the onset of emulsification, thereby increasing nanoparticle size upon emulsion maturation (Fig. 1A-B) [37]. Reducing the polymer amount allows polymer chains to envelop the drug more uniformly, creating denser cores that contribute to a smaller particle size [38]. These findings highlight the critical need to optimize key parameters, such as the polymer ratio and oil phase volume, to control nanoparticle size during formulation effectively.

The PDI is an essential parameter for characterizing particle size distribution, with values below 0.20 indicating a narrow distribution and a homogeneous dispersion [39]. In this study, the drug/polymer ratio (X1) was found to be the most significant variable affecting PDI, as it did particle size ($p < 0.05$) (Fig. 2A-B). The volume of the oil phase was also significant concerning the PDI ($p < 0.05$). As the oil phase volume (X3) increased, the PDI decreased, whereas expanding the polymer amount led to a higher PDI (Fig. 2B-C). In graphs where the drug/polymer ratio and the oil phase volume were fixed, sonication power (X2) did not significantly affect the PDI (Fig. 2A-C).

The findings of this study regarding the effects of polymer-drug ratio (X_1), sonication power (X_2), and oil-phase volume (X_3) on PDI are consistent with previous studies on PCL-based polymeric nanoparticles. Nawaz et al. (2021) showed that increasing the polymer content in PCL nanoparticles, optimized using a Box–Behnken design, significantly increased the PDI, confirming our findings that PDI increases with increasing X1 [40]. Similarly, Lima et al. (2023) showed that the oil phase/external aqueous phase volume ratio is a determinant of emulsion droplet formation and distribution, and that increasing the external phase volume can contribute to a reduction in PDI by promoting more homogeneous droplet formation; this explains the inverse relationship between X_3 and PDI [41]. The literature also emphasizes that the observed increase in PDI, depending on the amount of polymer, may be related to the difficulty of droplet fragmentation due to changes in the rheological properties of the organic phase [42]. In contrast, findings regarding sonication power indicate that ultrasonic energy can be a secondary determinant of PDI, and its effect may be limited when polymer amount and phase volumes are kept constant [25, 43].

The model demonstrated a high F-value (7.09) and a low p-value (0.0039), confirming its statistical significance, while the high R^2 value indicated a strong correlation between the experimental and predicted responses. These findings confirm that the selected linear model adequately fits the experimental data, and the mathematical regression equation describing this relationship is presented in Table 3. The statistical adequacy of the created models was evaluated using ANOVA analysis.

The EE% of PRX-loaded polymeric nanoparticles ranged from 69% to 90%, and statistical analyses indicated that the quadratic model best fit the data ($p < 0.05$). The high R^2

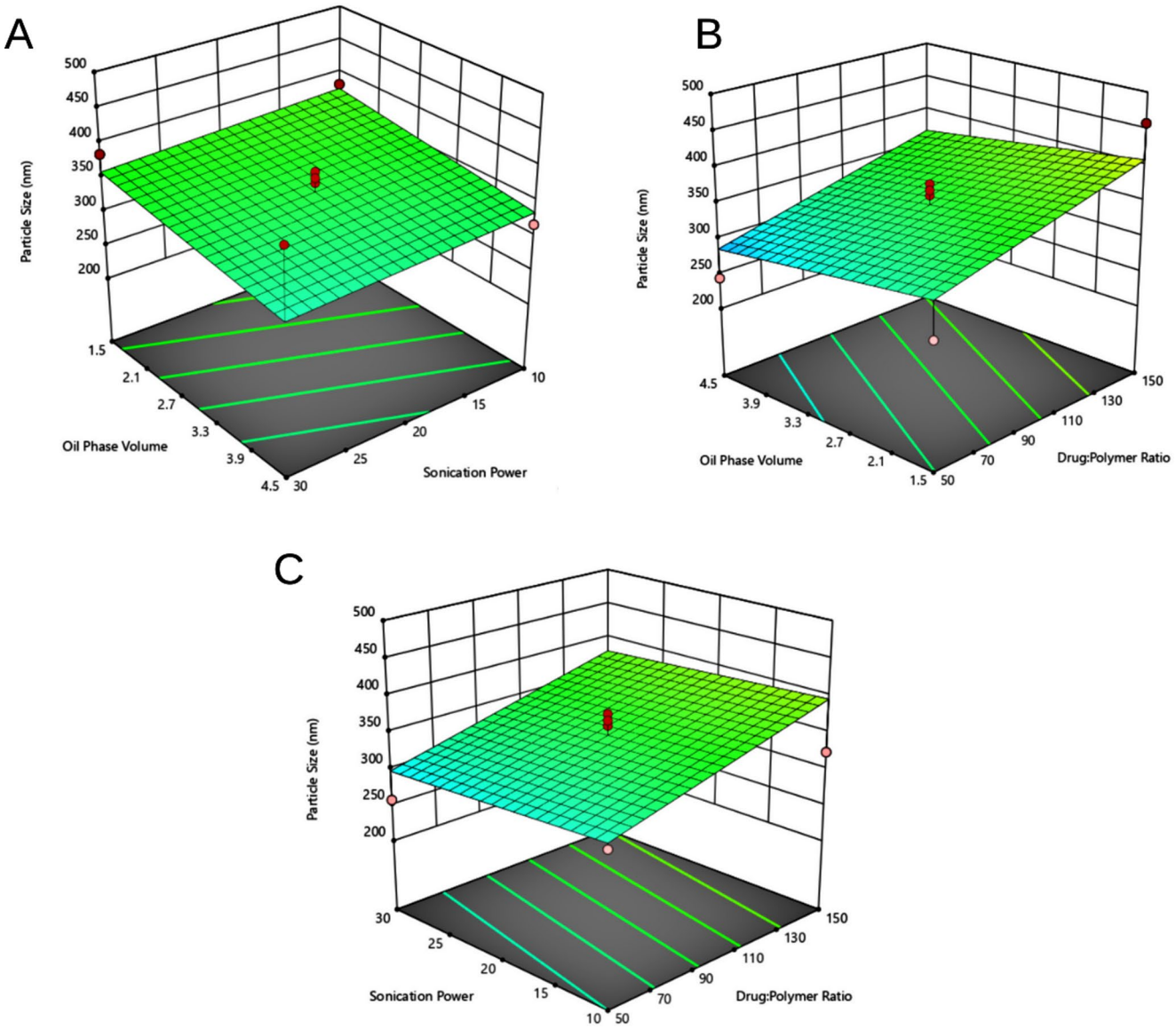


Fig. 1 3D response surface plots (**A**) Impact of polymer concentration and oil phase volume on particle size. (**B**) Impact of oil phase volume and drug/polymer ratio on particle size and (**C**) Impact of sonication power and drug/polymer ratio on particle size

Table 3 Statistical analysis and mathematical equations of dependent variables obtained from the box–behnken experimental design

Dependent variable	F Value	*p* Value	Mathematical equation
PS	2.96	0.0684	$0.819506X_1 - 0.815803X_2 - 13.39515X_3 + 321.42208$
PDI	7.09	0.0039	$0.001506X_1 - 0.002831X_2 - 0.069421X_3 + 0.388769$
EE%	7.59	0.0045	$0.449230X_1 - 1.82185X_2 + 16.37262X_3 - 0.000548X_1X_2 + 0.038481X_1X_3 + 0.003862X_2X_3 - 0.001796X_1^2 + 0.045460X_2^2 - 2.15735X_3^2 + 63.36401$
Dissolution of 12th hour (%)	5.93	0.0079	$0.287601X_1 + 0.892598X_2 + 15.11890X_3 - 31.41114$

value indicated strong agreement between the experimental results and the model predictions and demonstrated that the selected model reliably described the relationship between EE% and formulation parameters (Table 3).

Model outputs indicate that the drug-to-polymer ratio plays a decisive role in encapsulation efficiency. Increasing the polymer content to a threshold can enhance EE% by limiting the diffusion of the active substance into the external phase in emulsion-solvent evaporation-based systems; however, excessive increases in the polymer ratio can create diffusion constraints due to increased density within the particle matrix, thereby limiting the loading gain. This

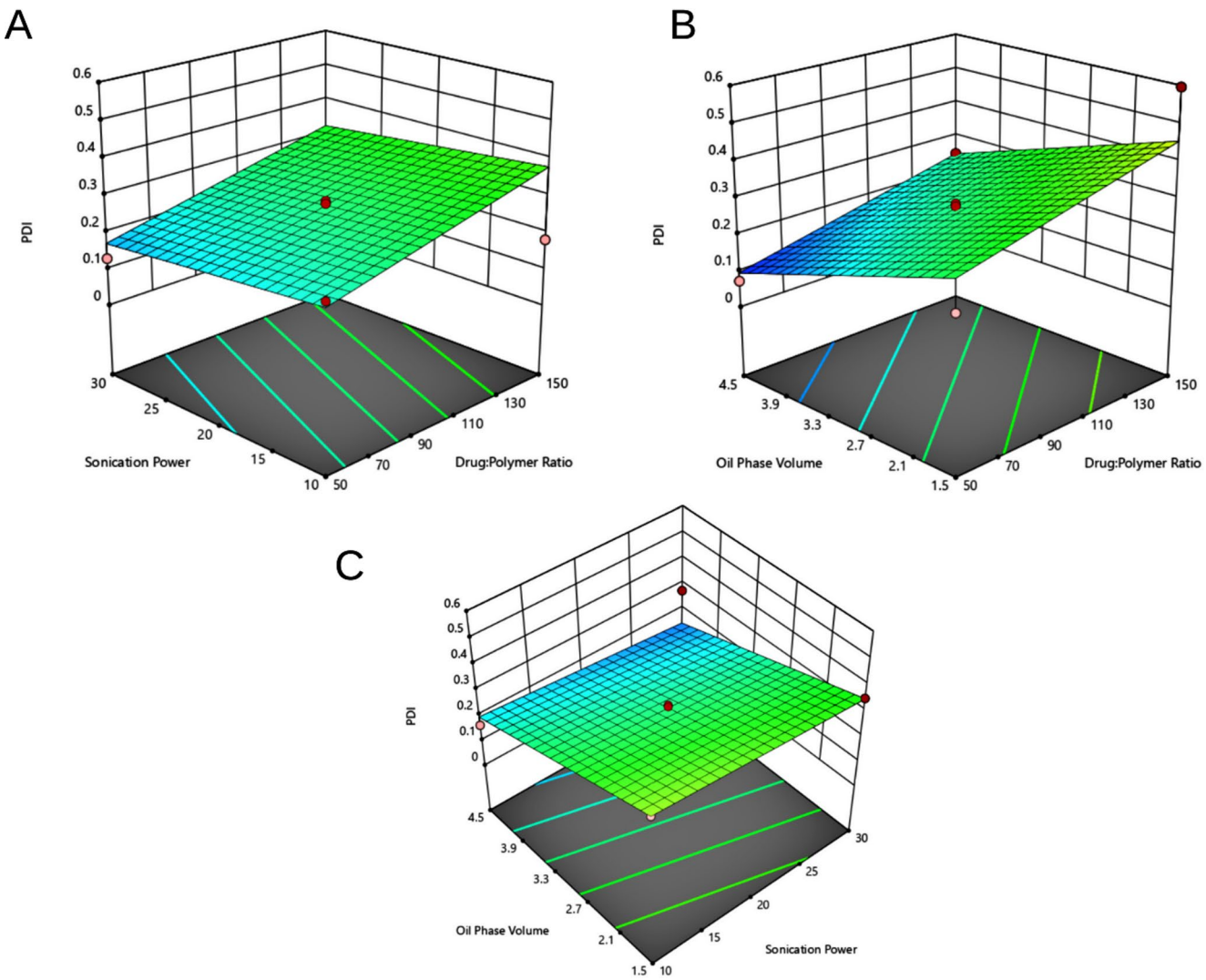


Fig. 2 3D response surface plots (**A**) Impact of sonication power and drug/polymer ratio on PDI. (**B**) Impact of oil phase volume and drug/polymer ratio on PDI and (**C**) Impact of oil phase volume and sonication power on PDI

"optimum range" profile is consistent with studies indicating that the amount of polymer in PCL nanoparticles increases encapsulation efficiency up to a certain point; however, at higher polymer contents, the additional increase in encapsulation efficiency is limited [44–46] (Fig. 3A-C).

The volume of the oil phase is one of the main formulation parameters that directly affects the encapsulation efficiency of the drug within the polymer matrix by determining the formation and breakup processes of droplets during emulsification. It has been reported that adjusting the oil phase volume in PCL nanoparticles has significant effects on the stability of droplets and the level of drug entrapment within the polymer matrix; medium oil phase volumes can support more regular and homogeneous droplet formation, thereby increasing encapsulation efficiency [47, 48]. Similarly, it is emphasized that optimizing the oil phase volume plays a critical role in enhancing encapsulation efficiency in other emulsion-based polymeric systems [49] (Fig. 3B-C).

From the perspective of sonication power, ultrasonic energy can have a dual effect on encapsulation efficiency. While moderate levels of ultrasonic energy reduce droplet size and thereby increase loading efficiency by activating emulsification, excessive energy application can weaken the integrity of the carrier structure and lead to drug loss from the particle surface. The literature emphasizes that sonication power must be kept within a formulation-specific optimal range. Our study's findings align with this "optimal range" approach [50, 51] (Fig. 3A-B).

Regarding the drug release profile, it has been observed that formulation parameters have significant effects on the percentage of drugs released after 12 h ($p < 0.05$). Especially, the amount of polymer is among the key variables

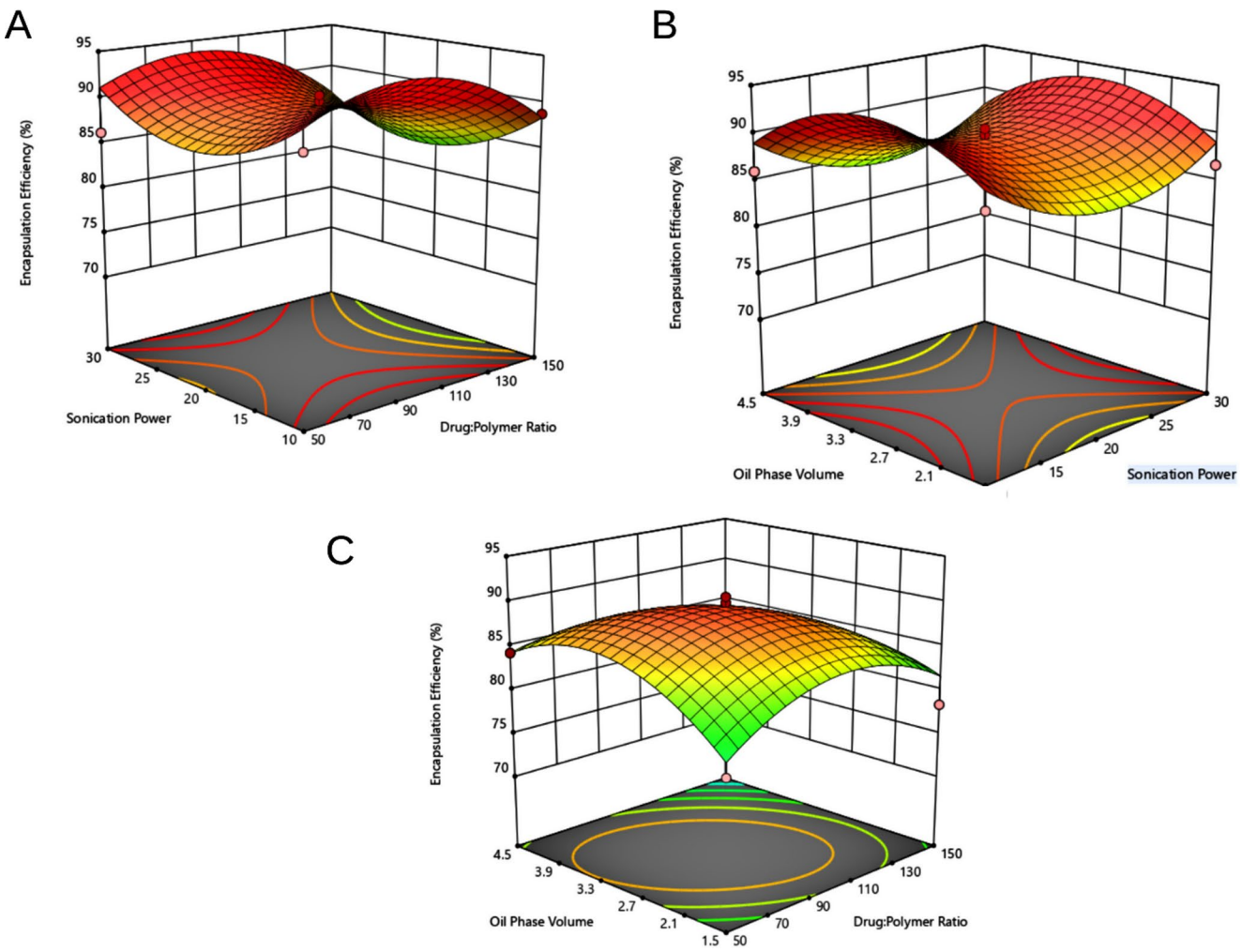


Fig. 3 3D response surface plots (**A**) Impact of sonication power and drug/polymer ratio on EE%. (**B**) Impact of oil phase volume and sonication power on EE% and (**C**) Impact of oil phase volume and drug/polymer ratio on EE%

determining the release kinetics. The literature indicates that increasing the polymer content results in a thicker, more hydrophobic polymer matrix. These modifications lead to an elongated diffusion pathway and a diminished initial release, ultimately facilitating a more continuous, controlled release profile [47, 52, 53]. Research indicates that in PCL-based systems, an increased polymer content improves long-term release stability and reduces the duration of the initial release phase [54, 55] (Fig. 4B-C).

When evaluated in terms of oil phase volume, it has been reported that the organic phase volume indirectly determines the release profile by changing the emulsion droplet size and particle morphology; an appropriate oil phase volume supports more homogeneous particle formation, and these structural differences are reflected in the release rate [48, 53, 56] (Fig. 4A-C).

The sonication power, rather than being a parameter that directly determines the release mechanism, primarily affects the release behavior secondarily by influencing particle size and surface area. Indeed, it has been reported that sonication time reduces the particle size of PCL nanoparticles. Still, the release rate is primarily determined by the amount of polymer and the properties of the carrier matrix [57]. However, excessive ultrasonic processing has been reported to weaken the integrity of the carrier structure and reduce encapsulation efficiency [43, 58] (Fig. 4A-B).

Zeta potential (ZP) is an indicator of the surface charge related to the colloidal stability of polymeric nanoparticles and their interactions with cells [59]. The PRX-loaded nanoparticles developed in this study exhibited zeta potential values ranging from − 2.15 to + 0.95 mV, indicating that the formulations generally possess a neutral/slightly charged surface character (Table 4). This finding suggests that in the respective systems, colloidal stability can be achieved through steric stabilization rather than electrostatic repulsion. In the literature, it is observed that nano-carriers

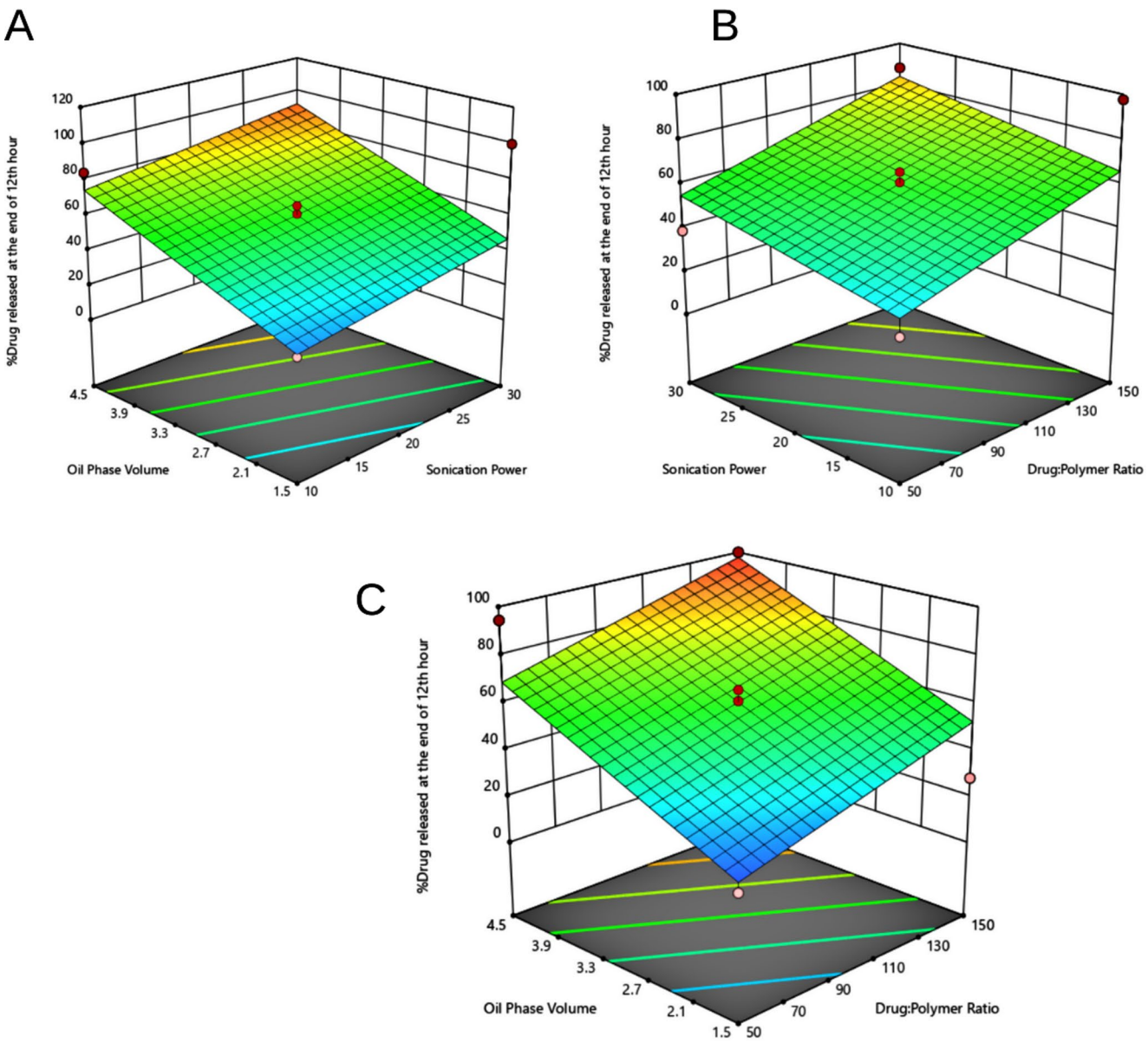


Fig. 4 3D response surface plots (**A**) Impact of oil phase volume and sonication power on % drug released at the end of the 12th hour. (**B**) Impact of sonication power and drug/polymer ratio on % drug released at the end of the 12th hour and (**C**) Impact of oil phase volume and drug/polymer ratio on % drug released at the end of the 12th hour

Table 4 Zeta potential values of PRX-loaded nanoparticle formulations (mean ± SD)

Code	ZP (mV) ± SD	Code	ZP (mV) ± SD
PRX1	-0.596 ± 0.081	PRX11	-0.173 ± 0.160
PRX2	-0.125 ± 0.110	PRX12	-1.270 ± 0.132
PRX3	0.101 ± 0.078	PRX13	0.503 ± 0.137
PRX4	0.566 ± 0.209	PRX14	-0.599 ± 0.049
PRX5	0.902 ± 0.606	PRX15	-2.150 ± 0.219
PRX6	-0.507 ± 0.165	PRX16	-0.610 ± 0.082
PRX7	-0.195 ± 0.265	PRX17	-1.050 ± 0.121
PRX8	0.946 ± 0.223	PRX18	-1.920 ± 0.140
PRX9	-0.209 ± 0.041	PRX19	-0.455 ± 0.102
PRX10	0.002 ± 0.142		

with zeta potentials close to neutral values can be sterically stabilized by non-ionic surfactants or polymeric coatings, thereby demonstrating long-term physical stability [60, 61].

In this study, the PRX-loaded polymeric nanoparticles formulation was optimized using Design-Expert® 7.0 software, and ANOVA confirmed the model's statistical significance. The relationships between the defined independent and dependent variables were mathematically expressed, and all models were found to be significant at the 95% confidence level ($p < 0.05$).

The targeted criteria for the optimization process were minimum particle size and PDI, maximum EE%, and release

Table 5 Statistical analysis and mathematical equations of dependent variables obtained from the box–behnken experimental design

Independent Variables	Dependent Variables	Experimental Result	Predicted Result	Error of prediction %
X1 (100:1)	Y1	304.1 ± 1.768	318.935	4.65
X2 (30 W)	Y2	0.143 ± 0.014	0.144	0.69
X3 (4.5 ml)	Y3	88 ± 0.129	88	0.15
PRX 3	Y4	78 ± 0.112	92	15.21

profile (Table 1). The calculated desirability function value for the optimum formulation obtained with a 1:100 drug/polymer ratio, 30 W sonication power, and 4.5 mL oil phase volüme was 0.829. The difference between the experimental results of this formulation and the model predictions was low, with errors of 4.65% for particle size, 0.69% for PDI, 0.15% for EE%, and 15.21% for the amount of active ingredient released at 12 h (Table 5).This optimized formulation was deemed the final composition, and all subsequent experimental evaluations were conducted with it. The high F-values and low p-values of the model demonstrated a strong fit between the established mathematical equations and the data. Thus, the obtained results indicate that the selected formulation parameters play a critical role in achieving the targeted properties in PRX-loaded polymeric nanoparticle systems, with linear and quadratic interactions contributing significantly. Overall, these findings confirm the robustness of the optimization strategy and justify selecting the optimized formulation for subsequent experimental evaluations.

In vitro Drug Release Studies of Optimum Formulations

To simulate the physiological environments of the gastrointestinal tract, in vitro drug release from the optimized PRX-loaded polymeric nanoparticles was investigated in buffer solutions at pH 1.2, 4.5, and 7.4. At pH 1.2, a rapid release occurred within the first 2 h, with cumulative release exceeding 30% (Fig. 5). The release rate further increased at pH 4.5 during the 2–4 h period, reaching over 70%. This initial burst release is attributed to the rapid diffusion of free or weakly polymer-bound drug molecules located at or near the nanoparticle surface. At later stages, the slower release phase observed at pH 7.4 over the 4–24 h period, approaching complete release, could be associated with the gradual erosion of the polymer matrix and the sustained diffusion pathways. Such a biphasic release profile is advantageous for maintaining therapeutic levels at the targeted colonic site and ensuring prolonged efficacy.

Drug release from optimized PRX-loaded polymeric nanoparticles has shown a biphasic release model (Fig. 5). In the initial phase, a faster release profile was observed, especially in pH 1.2 and 4.5 environments, with cumulative release exceeding 70% by the end of the first 4 h. It is thought that the rapid release initially observed is due to the rapid diffusion of free or loosely bound drug molecules located on or near the nanoparticle surface. In the literature, it has been reported that similar burst release behaviors were observed in PCL-based polymeric nanoparticles prepared by the double emulsion-solvent evaporation method, and this was particularly associated with drug molecules adsorbed on the surface [62]. In the subsequent phase, a more controlled and slower release profile was observed in a pH 7.4 environment over 4–24 h. It is thought that this situation is related to the hydrophobic structure of the PCL polymer, its slow degradation kinetics, and the extended diffusion pathways within the polymer matrix [63, 64] Similarly, the literature indicates that PCL-based nanoparticle systems can provide prolonged and controlled drug release [65, 66]. The two-phase release behavior observed is believed to offer

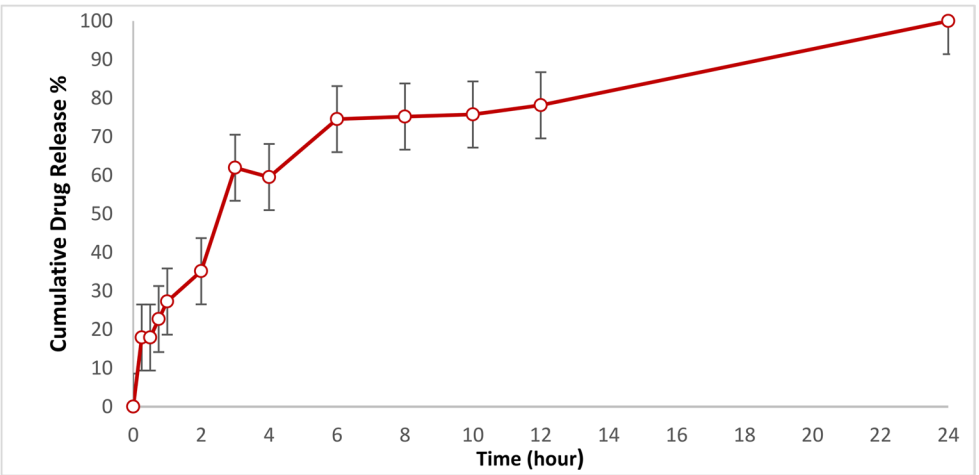


Fig. 5 Cumulative drug release profile (%) of PRX from the optimum PRX 3 coded formulation in a three-stage pH environment (0–2 h: pH 1.2, 2–4 h: pH 4.5, 4–24 h: pH 7.4)

Table 6 Evaluation of the drug release kinetics of optimized PRX-loaded polymeric nanoparticle formulation

Kinetic Parameters	Zero order	First order	Higuchi	Korsmeyer-Peppas
k	5.991	0.224	24.340	32.669
r^2	0.847	0.978	0.959	0.975
RMS	28.074	8.9526	10.119	7.183
n	-	-	-	0.371

k release rate constant, *n* diffusional exponent coefficient, r^2correlation coefficient, *RMS* Residual mean square

an advantage for colon-targeted drug delivery systems by allowing for a rapid attainment of the therapeutic effective concentration initially, followed by a sustained release of the drug over an extended period [67, 68]. k: release rate constant; n: diffusional exponent coefficient; r^2: correlation coefficient; RMS: Residual mean square. The drug release profile of the optimized PRX-loaded polymeric nanoparticle formulation was evaluated using zero-order, first-order, Higuchi, and Korsmeyer–Peppas kinetic models (Table 6). When the drug release kinetics were examined, it was determined that the release profile showed the best fit to the first-order kinetic model with the highest correlation coefficient (r^2=0.978) and a low RMS value. Additionally, it was observed that the correlation coefficient of the Korsmeyer–Peppas model was also high (r^2=0.975). The release exponent value (n=0.371) calculated according to the Korsmeyer–Peppas model indicates that the release mechanism is Fickian diffusion-controlled. These results suggest that PRX is released from the polymeric matrix thru a controlled diffusion mechanism.

Morphology of Optimized PRX-Loaded Polymeric Nanoparticle Formulation

TEM analysis was performed to examine the morphological properties of PRX-loaded polymeric nanoparticles. As seen in Fig. 6, it has been determined that the nanoparticles have a spherical shape and exhibit a homogeneous distribution. Additionally, it has been evaluated that the obtained morphological findings are consistent with the particle size distribution obtained from dynamic light scattering analyzes.

Evaluation of the Stability of the Optimized Polymeric Nanoparticles

Storage conditions can affect the stability of nanoparticle drug delivery systems. Therefore, in our study, the effects of storage conditions were investigated by comparing the initial and 3-month physicochemical properties of optimized PRX-loaded polymeric nanoparticles. According to the results in Table 7, it was determined that none of the examined properties showed a statistically significant change compared to the initial values after 3 months ($p>0.5$) .

Cytotoxicity Evaluation

HCT116, a human CRC cell line, was used for the assessment of the antiproliferative activity of the free drug and drug-loaded optimized nanoformulation. For this purpose, seven doses of free drug and six doses of drug-loaded nanoformulation were applied to the cells for incubation periods of 24, 48 and 72 h. As shown in Fig. 7, the viability of HCT-116 cells decreased in a time- and dose-dependent manner after both free PRX and PRX-loaded nanoformulation treatment. Free PRX reduced cellular viability significantly between 3.906 and 15.625 µg/ml concentration range ($p<0.0001$) following 24 h incubation; 1.953–15.625 µg/ml ($p<0.0001$) and 0.977 µg/ml ($p<0.01$) following 48 h incubation; 0.977–15.625 µg/ml ($p<0.0001$) and 0.244–0.488 µg/ml ($p<0.01$) following 72 h incubation (Fig. 7a). PRX-loaded nanoformulation decreased cell viability

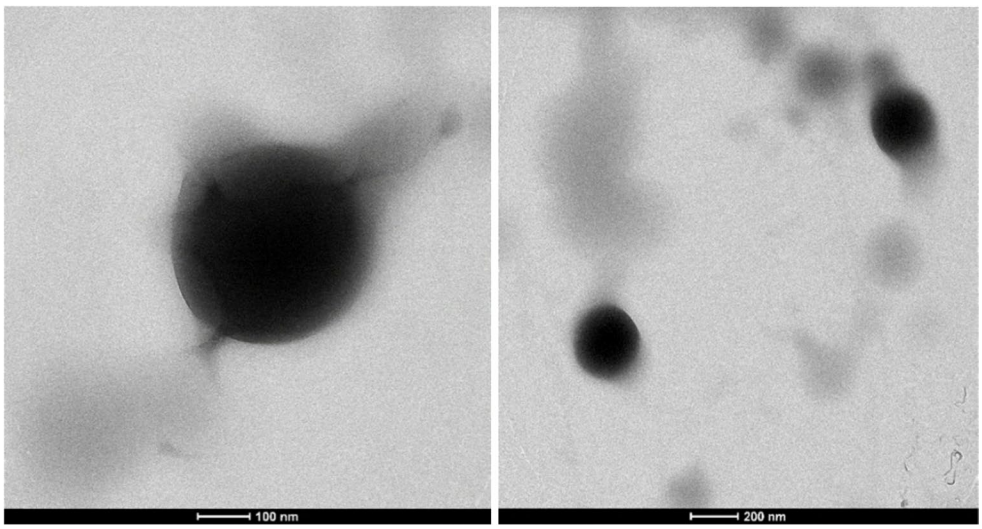


Fig. 6 TEM images of optimum PRX-3 coded nanoparticles formulation

Table 7 Evaluation of the stability studies of the optimized polymeric nanoparticles

	PS (nm) ± SD	PDI ± SD	ZP (mV) ± SD
Initial	304.1 ± 1.768	0.143 ± 0.014	0.101 ± 0.078
Month 3	304.6 ± 1.504	0.151 ± 0.017	0.303 ± 0.205

significantly at 15.625 µg/ml ($p < 0.001$) after 24 h incubation and following 24 and 48 h incubation it decreased significantly between 0.488 and 15.625 µg/ml concentration range ($p < 0.0001$) (Fig. 7b). It was observed that the IC50 values of free PRX decreased in a time dependent manner (14.505 ± 1.652 µg/ml; 10.937 ± 0.7697 µg/ml; 7.21 ± 0.743 µg/ml for 24, 48 and 72 h respectively). Similarly, a decrease in IC50 values was observed in a time dependent manner in the PRX-loaded nanoformulation (12.86 ± 1.41 µg/ml; 1.614 ± 0.733 µg/ml; 1.6 ± 0.431 µg/ml for 24, 48 and 72 h respectively). When comparing the IC50 values of free PRX and PRX-loaded nanoformulation, the IC50 values of PRX-loaded nanoformulation were found to be lower than those of free PRX after all incubation periods of 24, 48 and 72 h (Table 8).

This instance has shown that drug-loaded nanoparticles have a more pronounced antiproliferative effect compared to free drugs. It is thought that the obtained efficacy may be related to the increased cellular uptake of nanoparticles and their controlled release properties [69, 70]. It has also been reported in the literature that PCL-based nanoparticle systems can enhance cellular transport and strengthen

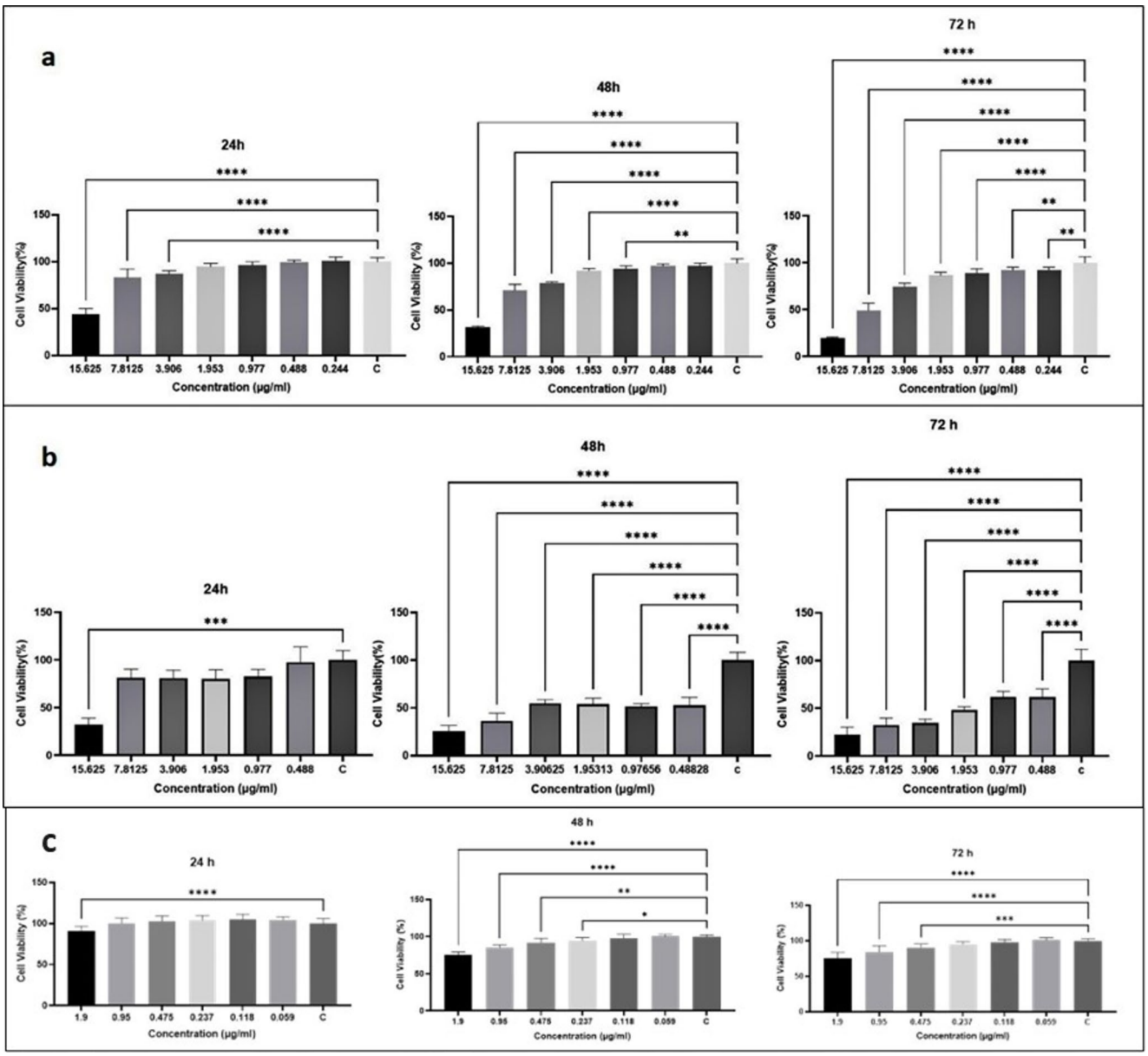


Fig. 7 Cytotoxic activity profiles of (**a**) free PRX and (**b**) optimum PRX 3 coded nanoparticles formulation (**c**) blank nanoparticle

Table 8 IC50 value of free PRX and PRX-loaded nanoparticles against HCT-116 cells at 24, 48 and 72 h

IC50 (µg/ml)	24 h	48 h	72 h
Free Paroxetine	14.505 ± 1.652	10.937 ± 0.7697	7.21 ± 0.743
Optimum Paroxetine loaded polymeric nanoparticle (PRX 3)	12.86 ± 1.41	1.614 ± 0.733	1.6 ± 0.431

anticancer efficacy [71, 72]. Additionally, it is stated that in nanoparticle systems providing controlled release, the cytotoxic effect becomes more pronounced as the incubation period is extended [73]. Overall, the results indicate that PRX-loaded nanoparticles can enhance antiproliferative activity in HCT-116 cells, particularly with prolonged incubation periods.

The biocompatibility of blank nanoparticle formulations was evaluated in the HCT-116 cell line. At a concentration of 1.9 µg/ml, cell viability was determined to be 90.93 ± 5.716% at 24 h, 75.61 ± 3.66% at 48 h, and 75.05 ± 8.55% at 72 h. Moreover, even at the highest concentration, cell viability did not fall below 75%. The findings have been evaluated according to the ISO 10993-5 standard. According to the relevant standard, a cell viability below 70% is considered an indicator of cytotoxicity. Therefore, the blank nanoparticle formulations have been evaluated as biocompatible. (Fig. 7)

Conclusion

In this study, paroxetine-loaded polymeric nanoparticle formulations were developed and optimized using a Box–Behnken experimental design. Under the optimized formulation conditions (drug/polymer ratio 1:100, sonication power 30 W, oil phase volume 4.5 mL), the polymeric nanoparticles exhibited a mean particle size of 304.1 ± 1.76 nm, a PDI of 0.143 ± 0.014, an EE of 88%, and 78% drug release after 12 h. The low error of prediction values between the experimental data and the model predictions confirmed the reliability of the developed model. Furthermore, cytotoxicity analyses performed on the HCT-116 colon cancer cell line demonstrated that these formulations produced more pronounced antiproliferative effects compared with free PRX. Overall, these findings suggest that the optimized polymeric nanoparticle system achieved favorable physicochemical properties, including an appropriate particle size, narrow size distribution, high encapsulation efficiency and sustained drug release behavior. More importantly, the enhanced antiproliferative activity of the nanoparticle formulation indicates its potential as a promising drug delivery platform for colorectal cancer therapy. However, further in vivo studies using appropriate colorectal cancer models are planned to validate these in vitro findings and to further assess the therapeutic potential of the developed formulation.

Acknowledgements This research was supported by The Scientific and Technological Research Council of Türkiye (TUBITAK), with grant no: 124S705.

Author Contributions Conceptualization: C.H., O.E., S.D., Methodology: C.H., O.E., S.D., Formal analysis and investigation: S.D., A.K., Writing-original draft preparation: C.H., O.E., S.D., A.K., Writing-review and editing: C.H., O.E., S.D., Supervision: C.H.

Funding Open access funding provided by the Scientific and Technological Research Council of Türkiye (TÜBİTAK). Declaration. This research was supported by The Scientific and Technological Research Council of Türkiye (TUBITAK), with grant no: 124S705.

Data Availability No datasets were generated or analysed during the current study.

Declarations

Competing Interests The authors declare no competing interests.
The authors have no competing interests to declare that are relevant to the content of this article.

Open Access This article is licensed under a Creative Commons Attribution 4.0 International License, which permits use, sharing, adaptation, distribution and reproduction in any medium or format, as long as you give appropriate credit to the original author(s) and the source, provide a link to the Creative Commons licence, and indicate if changes were made. The images or other third party material in this article are included in the article's Creative Commons licence, unless indicated otherwise in a credit line to the material. If material is not included in the article's Creative Commons licence and your intended use is not permitted by statutory regulation or exceeds the permitted use, you will need to obtain permission directly from the copyright holder. To view a copy of this licence, visit http://creativecommons.org/licenses/by/4.0/.

References

1. Shaham S, Vij P, Tripathi M. Advances in targeted and chemotherapeutic strategies for colorectal cancer: current insights and future directions. Biomedicines. 2025;13(3):642.
2. Siegel RL, Wagle NS, Star J, Kratzer TB, Smith RA, Jemal A. Colorectal cancer statistics, 2026. CA Cancer J Clin. 2026;76(2):e70067.
3. Guo Y, Wang M, Zou Y, Jin L, Zhao Z, Liu Q, Wang S, Li J. Mechanisms of chemotherapeutic resistance and the application of targeted nanoparticles for enhanced chemotherapy in colorectal cancer. J Nanobiotechnol. 2022;20(1):433.

4. Chen W, Shi K, Yu Y, Yang P, Bei Z, Mo D, Yuan L, Pan M, Chen Y, Qian Z. Drug delivery systems for colorectal cancer chemotherapy. Chin Chem Lett. 2024;34(1):109159.
5. Was H, Borkowska A, Bagues A, Tu L, Liu JYH, Lu Z, Rudd JA, Nurgali K, Abalo R. Mechanisms of chemotherapy-induced neurotoxicity. Front Pharmacol. 2022;13:750507.
6. He Y, Zheng J, Ye B, Dai Y, Nie K. Chemotherapy-induced gastrointestinal toxicity: pathogenesis and current management. Biochem Pharmacol. 2023;216:115787.
7. Chai M, Wang S, Chen Y, Pei X, Zhen X. Targeted and intelligent nano-drug delivery systems for colorectal cancer treatment. Front Bioeng Biotechnol. 2025;13:1582659.
8. Kumar A, Vaiphei KK, Singh N, Chigurupati SPD, Paliwal SR, Paliwal R, Gulbake A. Nanomedicine for colon-targeted drug delivery: strategies focusing on inflammatory bowel disease and colon cancer. Nanomed (Lond). 2024;19(15):1347–68.
9. Gouveia M, Ribeiro E, Vale N. A surprising repurposing of central nervous system drugs against squamous cell carcinoma of the bladder UM-UC-5. Pharmaceutics. 2024;16(2):212.
10. Bardaweel S, Jaradat E, Hajjo R, AlJarrah H. Unraveling the anticancer potential of SSRIs in prostate cancer by combining computational systems biology and in vitro analyses. ACS Omega. 2025;10(15):15204–18.
11. Gül S, Aydemir E. The use of selective serotonin reuptake inhibitor antidepressants in the treatment of lung cancer. Int J Mol Sci. 2025;26(10):4546.
12. He L, Fu Y, Tian Y, Wang X, Zhou X, Ding R, Qi X, Bao J. Antidepressants as autophagy modulators for cancer therapy. Molecules. 2023;28(22):7594.
13. Blum C, Dohrmann M, McCarthy L, McMenamin M, O'Callaghan L. Repurposing the antidepressant sertraline: a systematic scoping review of its anticancer mechanisms. Pharmacol Res Perspect. 2025;13:e70168.
14. Davis BA, Chen A, Rudnick G. Mechanism of paroxetine (Paxil) inhibition of the serotonin transporter. Sci Rep. 2016;6:23789.
15. Kowalska M, Piłat A, Błasiak J, Sobolewski M. Assessment of paroxetine molecular interactions with selected transporters. Int J Mol Sci. 2021;22(12):6293.
16. Huang Q, Wu M, Pu Y, Zhou J, Zhang Y, Li R, Xia Y, Zhang Y. Inhibition of TNBC cell growth by paroxetine: induction of apoptosis and blockage of autophagy flux. Cancers. 2024;16(5):885.
17. Cho Y, Kim E, Nyiramana M, Shin E, Jin H, Ryu J, Kang K, Lee G, Kim H, Han J, Kang D. Paroxetine induces apoptosis of human breast cancer MCF-7 cells through Ca^{2+}- and p38 MAP kinase-dependent ROS generation. Cancers. 2019;11(1):64.
18. Jang WJ, Jung SK, Tam V, Jeong C-H. Anticancer activity of paroxetine in human colon cancer cells. Biomol Ther (Seoul). 2019;27(3):282–9.
19. Wang K, Gong Q, Zhan Y, Chen B, Yin T, Lu Y, Zhang Y, Wang H, Ke J, Du B, Liu X, Xiao J. Blockage of autophagic flux and induction of mitochondria fragmentation by paroxetine hydrochloride in lung cancer cells promotes apoptosis via the ROS-MAPK pathway. Front Cell Dev Biol. 2020;7:397.
20. Liu BH, Yuan TM, Huang CJ. DNA repair proteins as targets for paroxetine-induced cytotoxicity in gastric cancer AGS cells. Am J Cancer Res. 2022;12(4):1465–83.
21. Elshafeey A, El-Dahmy R. Formulation and development of oral fast-dissolving films loaded with nanosuspension to augment paroxetine bioavailability: in vitro characterization, ex vivo permeation, and pharmacokinetic evaluation in healthy human volunteers. Pharmaceutics. 2021;13(11):1869.
22. Rüdesheim S, Selzer D, Mürdter TE, Igel S, Kerb R, Schwab M, Lehr T. Physiologically based pharmacokinetic modeling to describe the CYP2D6 activity score-dependent metabolism of paroxetine, atomoxetine and risperidone. Pharmaceutics. 2022;14(8):1734.
23. Song Y, Yang X, Yu B. Repurposing antidepressants for anticancer drug discovery. Drug Discov Today. 2021;26(12):2912–23.
24. Raza M, Sharma M, Nagori K, Jain P, Ghosh V, Gupta U, Uddin A. Recent trends on polycaprolactone as sustainable polymer-based drug delivery system in the treatment of cancer: Biomedical applications and nanomedicine. Int J Pharm. 2024;666:124734.
25. Iqbal M, Valour JP, Fessi H, Elaissari A. Preparation of biodegradable PCL particles via double emulsion evaporation method using ultrasound technique. Colloid Polym Sci. 2015;293:861–73.
26. Czyrski A, Jarzębski H. Response surface methodology as a useful tool for evaluation of the recovery of the fluoroquinolones from plasma: the study on applicability of Box–Behnken design, central composite design and Doehlert design. Processes. 2020;8(4):473.
27. Yadav P, Rastogi V, Verma A. Application of Box–Behnken design and desirability function in the development and optimization of self-nanoemulsifying drug delivery system for enhanced dissolution of ezetimibe. Future J Pharm Sci. 2020;6:7.
28. Szpisják-Gulyás N, Al-Tayawi AN, Horváth ZH, László Z. Kertész Sz, Hodúr C. Methods for experimental design, central composite design and the Box–Behnken design to optimise operational parameters: a review. Acta Aliment. 2023;52(4):521–37.
29. Rekha SM, Sangeetha S. Formulation design, optimization, and evaluation of solid lipid nanoparticles loaded with an antiviral drug tenofovir using Box–Behnken design for boosting oral bioavailability. Adv Pharmacol Pharm Sci. 2024;2024:5248746.
30. Simsek E, Esim O, Hascicek C. Paroxetine HCl-loaded hybrid nanoparticles for intranasal application to brain delivery: evaluation and cell culture studies. J Nanopart Res. 2025;27:214.
31. Sengel-Turk CT, Hascicek C. Design of lipid–polymer hybrid nanoparticles for therapy of BPH: Part I. Formulation optimization using a design of experiment approach. J Drug Deliv Sci Technol. 2017;39:16–27.
32. Ravisankar P, Roja C, Kishore Babu G, Sai Rahul K. Validated UV spectrophotometric method for quantitative analysis of paroxetine in bulk and pharmaceutical dosage form. Der Pharma Chem. 2014;6(2):188–92.
33. Esim O, Kiymaci ME, Hascicek C. Ciprofloxacin HCl-loaded albumin nanoparticles for the treatment of recurrent urinary tract infections: preparation, optimization, and evaluation of antibacterial activity. J Pharm Innov. 2023;18(3):1100-1110.
34. Zhang Y, Huo M, Zhou J, Zou A, Li W, Yao C, Xie S. DDSolver: an add-in program for modeling and comparison of drug dissolution profiles. Aaps j. 2010;12(3):263–71.
35. Khayat MT, Zarka MA, El-Telbany DFA, Al Saqr A, Alshahrani SM, Abu-Dief AM, Alshahrani MY. Intensification of resveratrol cytotoxicity, pro-apoptosis, oxidant potentials in human colorectal carcinoma HCT-116 cells using zein nanoparticles. Sci Rep. 2022;12:15235.
36. Zielińska A, Carreiró F, Oliveira AM, Neves A, Pires B, Venkatesh DN, Durazzo A, Lucarini M, Eder P, Silva AM, Santini A, Souto EB. Polymeric nanoparticles: production, characterization, toxicology and ecotoxicology. Molecules. 2020;25(16):3731.
37. Crucho CIC, Barros MT. Polymeric nanoparticles: a study on the preparation variables and characterization methods. Mater Sci Eng C. 2017;80:771–84.
38. Beirampour N, Minaei A, Varshosaz J. Formulation of polymeric nanoparticles loading baricitinib: effects of polymer, surfactant, and aqueous phase on particle size and PDI. Pharmaceutics. 2024;16(8):1092.
39. Esim O, Gedik ME, Doğan AL, Günaydın G, Hasçiçek C. Development of carboplatin loaded bovine serum albumin nanoparticles and evaluation of its effect on an ovarian cancer cell line. J Drug Deliv Sci Technol. 2021;66:102655.
40. Nawaz T, Iqbal M, Khan B, Nawaz A, Hussain T, Hosny KM, Abualsunun W, Rizg W. Development and optimization of acriflavine-loaded polycaprolactone nanoparticles using

Box–Behnken design for burn wound healing applications. Polymers. 2022;14(1):101.
41. Lima T, de Silva de Oliveira M, Reis A, Petrilli R, Eloy JO. Nanoencapsulation of methylene blue for enhanced skin cancer cell phototoxicity and cutaneous penetration in association with sonophoresis. Pharmaceutics. 2023;15(5):1371.
42. Gilani SA, Bin-Jumah M, Fatima F. Development of statistically optimized piperine-loaded polymeric nanoparticles for breast cancer: in vitro evaluation and cell culture studies. ACS Omega. 2023;8(44):44183–94.
43. Ruiz E, Orozco V, Hoyos L, Giraldo L. Study of sonication parameters on PLA nanoparticles preparation by simple emulsion–evaporation solvent technique. Eur Polym J. 2022;170:111307.
44. Kamaraj N, Rajaguru P, Issac P, Sundaresan S. Fabrication, characterization, in vitro drug release and glucose uptake activity of 14-deoxy,11,12-didehydroandrographolide-loaded polycaprolactone nanoparticles. Asian J Pharm Sci. 2017;12(4):353–62.
45. Mahmoud B, McConville C. Box–Behnken design of experiments of polycaprolactone nanoparticles loaded with irinotecan hydrochloride. Pharmaceutics. 2023;15(4):1271.
46. Tekin T, Yıldız A, Demiröz F, Acartürk F. Optimization formulation of insulin-loaded poly-caprolactone nanoparticles for chronic wound healing using Box–Behnken design. J Fac Pharm Ankara Univ. 2025;49(3):900-914.
47. Ribeiro A, Rezende RO, Cabral LM, de Sousa VP. Poly(ε-caprolactone) nanoparticles loaded with *Uncaria tomentosa* extract: preparation, characterization, and optimization using Box–Behnken design. Int J Nanomed. 2013;8:431–42.
48. Sadoun-Daikha O, Rodríguez M, Azouz L, Rabasco AM, Rezgui F. Central composite design optimization for a controlled valsartan release from polycaprolactone microspheres. J Appl Polym Sci. 2021;138:e50631.
49. Song X, Zhao Y, Hou S, Xu F, Zhao R, He J, Cai Z, Li Y, Chen Q. Dual agents loaded PLGA nanoparticles: systematic study of particle size and drug entrapment efficiency. Eur J Pharm Biopharm. 2008;69(2):445–53.
50. Luo X, Fan F, Sun X, Li P, Xu T, Ding J, Fang Y. Effect of ultrasonic treatment on the stability and release of selenium-containing peptide-encapsulated nanoparticles in vitro and in vivo. Ultrason Sonochem. 2022;83:105923.
51. Alam M, Kassu A, Kassama L. Effect of surfactant and sonication time on improving the bioaccessibility of lycopene synthesized in poly(lactic-co-glycolic acid) nanoparticles. *ASABE Annu Int Meet Proc*. 2023.
52. Elmowafy M, Alruwaili N, Shalaby K, Alharbi K, Altowayan W, Ahmad N, Zafar A, Elkomy M. Long-acting paliperidone parenteral formulations based on polycaprolactone nanoparticles: influence of stabilizer and chitosan on in vitro release, protein adsorption, and cytotoxicity. Pharmaceutics. 2020;12(2):160.
53. Kumar A, Sawant KK. Encapsulation of exemestane in polycaprolactone nanoparticles: optimization, characterization, and release kinetics. Cancer Nanotechnol. 2013;4:57–71.
54. Al-Mohammedawi M, Mohsien R, Kadhim M, Bahjat E, Azawi D, Qaraghuli S. The release property of amoxicillin nanoparticles and their antibacterial activity. Nano Sci Nano Technol. 2019;13:1–16.
55. Samy M, Abdallah H, Ayoub M, Vylegzhanina M, Volkov A, Sukhanova T. Eco-friendly route for encapsulation of 5-fluorouracil into polycaprolactone nanoparticles. Egypt J Chem. 2020;63:255–63.
56. Nagy N, Varga Z, Mihály J, Kasza G, Iván B. Highly efficient encapsulation of curcumin into and pH-controlled drug release from poly(ε-caprolactone) nanoparticles stabilized with an amphiphilic hyperbranched polyglycerol. Express Polym Lett. 2020;14(1):90–101.
57. Badran M, Alanazi A, Ibrahim M, Alshora D, Taha E, Alomrani A. Optimization of bromocriptine-mesylate-loaded polycaprolactone nanoparticles coated with chitosan for nose-to-brain delivery: in vitro and in vivo studies. Polymers. 2023;15(19):3890.
58. Byun Y, Hwang J, Bang S, Darby D, Cooksey K, Dawson P, Park H, Whiteside S. Formulation and characterization of α-tocopherol-loaded poly(ε-caprolactone) nanoparticles. LWT Food Sci Technol. 2011;44(1):24–8.
59. Clogston JD, Patri AK. Zeta potential measurement. Methods Mol Biol. 2010;697:63–70.
60. Cortés H, Hernández-Parra H, Bernal-Chávez S, Prado-Audelo MLD, Caballero-Florán IH, Borbolla-Jiménez FV, González-Torres M, Magaña JJ, Leyva-Gómez G. Non-ionic surfactants for stabilization of polymeric nanoparticles for biomedical uses. Mater (Basel). 2021;14(12):3187.
61. Tran E, Richmond GL. Interfacial steric and molecular bonding effects contributing to the stability of neutrally charged nanoemulsions. Langmuir. 2021;37(43):12643–53.
62. Javaid S, Ahmad N, Mahmood A, Nasir H, Iqbal M, Ahmad N, Irshad S. Cefotaxime loaded polycaprolactone based polymeric nanoparticles with antifouling properties for in-vitro drug release applications. Polymers. 2021;13(13):2180.
63. Eltaib L. Polymeric nanoparticles in targeted drug delivery: Unveiling the impact of polymer characterization and fabrication. Polymers. 2025;17(7):833.
64. Kim Y, Kwak J, Lim M, Lim S, Chae S, Ha S, Won Y, Kim H, Lim K. Advances in PCL, PLA, and PLGA-based technologies for anticancer drug delivery. Pharmaceutics. 2025;17(10):1354.
65. Stiepel R, Pena E, Ehrenzeller S, Gallovic M, Lifshits L, Genito C, Bachelder E, Ainslie K. A predictive mechanistic model of drug release from surface eroding polymeric nanoparticles. J Control Release. 2022;351:1–12.
66. Deshmukh V, Narwade M, Gajbhiye K. Intranasal delivery of paclitaxel-loaded ligand conjugated polymeric nanoparticles for targeted brain delivery. AAPS PharmSciTech. 2025;26:46.
67. Naeem M, Choi M, Cao J, Lee Y, Ikram M, Yoon S, Lee J, Moon H, Kim M, Jung Y, Yoo J. Colon-targeted delivery of budesonide using dual pH- and time-dependent polymeric nanoparticles for colitis therapy. Drug Des Devel Ther. 2015;9:3789–99.
68. Turanlı Y, Acartürk F. Preparation and characterization of colon-targeted pH/time-dependent nanoparticles using anionic and cationic polymethacrylate polymers. Eur J Pharm Sci. 2022;181:106122.
69. Xiao X, Teng F, Shi C, Chen J, Wu S, Wang B, Meng X, Imeh A, Li W. Polymeric nanoparticles—promising carriers for cancer therapy. Front Bioeng Biotechnol. 2022;10:1024143.
70. Gagliardi A, Giuliano E, Venkateswararao E, Fresta M, Bulotta S, Awasthi V, Cosco D. Biodegradable polymeric nanoparticles for drug delivery to solid tumors. Front Pharmacol. 2021;12:601626.
71. Mady FM, Shaker MA. Enhanced anticancer activity and oral bioavailability of ellagic acid through encapsulation in biodegradable polymeric nanoparticles. Int J Nanomed. 2017;12:7405–17.
72. Sunoqrot S, Abusulieh S, Sabbah D. Polymeric nanoparticles potentiate the anticancer activity of novel PI3Kα inhibitors against triple-negative breast cancer cells. Biomedicines. 2024;12(12):2676.
73. Khan S, Madni A, Aamir M, Khan S, Ahmad F, Basit A, Jan N, Shah H, Shafiq A, Anwar M. Design and evaluation of sustained-release lipid–PLGA hybrid nanoparticles for enhanced anticancer efficacy of 5-fluorouracil. Part Sci Technol. 2024;42(3):269–87.

Publisher's Note Springer Nature remains neutral with regard to jurisdictional claims in published maps and institutional affiliations.